Volume xx (*200y*), *Number z, pp. 1–12*

Massless Cable for Real-time Simulation

M. Servin[1] and C. Lacoursière[2]

[1]Department of Physics, [2]HPC2N/VRlab and Dept. of Computing Science
Umeå University, SE-901 87 Umeå, SWEDEN

Abstract

A technique for real-time simulation of hoisting cable systems based on a multibody non-ideal constraint is presented. The hoisting cable constraint is derived from the cable internal energies for stretching and twisting. Each hoisting cable introduces two constraint equations, one for stretching and one for torsion, which include all the rigid bodies attached by the same cable. The computation produces the global tension and torsion in the cable as well as the resulting forces and torques on each attached body. The complexity of the computation grows linearly with the number of bodies attached to a given cable and is weakly coupled to the rest of the simulation. The non-ideal constraint formulation allows stable simulations of cables over wide ranges of linear and torsional stiffness, including the rigid limit. This contrasts with lumped element formulations including the cable internal degrees of freedom in which computational complexity grows at least linearly with the number of cable elements–usually proportional to cable length–and where numerical stability is sensitive to the mass ratio between the load and the lumped elements.

Categories and Subject Descriptors (according to ACM CCS): I.3.5 [Computer Graphics]: Physically based modeling
I.3.7 [Computer Graphics]: Virtual reality

1. Introduction

Stable and fast numerical integration of mechanical systems is an essential component of interactive, physics driven simulator systems, which are widely used in virtual environment heavy machinery operator training applications. Current research and development in this field focuses on developing physical models that are well adapted to the required level of detail of these applications, and the corresponding numerical methods suitable for the real-time requirements in stability, speed, and accuracy.

Real-time numerical integration of systems of constrained and contacting rigid bodies has reached some level of maturity and optimized software libraries are widely available for this problem. See Ref. [ESHD05] for an overview. Rigid multibody models are sufficient for a number of applications ranging from vehicle dynamics to bio-mechanical systems for instance. Constraints enforcing restrictions on the relative motion of a set of the rigid elements, are essential for producing useful models. Typical constraint libraries offer a whole range, from simple ball joints to a car-wheel assembly including suspension and steering. Constraints model the net geometric effect of dynamics on short time and length scales that is intractable to simulate directly. A hinge constraint for instance replaces much detailed contact physics with a simple kinematic condition on a pair of rigid bodies.

When the constraint forces are solved for explicitly using a first order linear approximation as done for instance in [Bar96] and [WGW90], constraint violation never exactly vanishes. At best, if a robust stabilization method is used, constraint violation exhibits *damped oscillation*. Using the physics-based stabilization scheme described in [Lac06] for instance, constraint relaxation dynamics can be used to extend rigid multibody modeling in the flexible regime. In what follows, we use the regularized integration scheme of [Lac06] in conjunction with a novel constraint definition to model the effect of a massless cable under tension joining a set of rigid bodies. The result is a model of a hoisting cable which connects a set of rigid bodies–which may also be otherwise constrained–via a *fixture*, defined as a reference frame rigidly attached to a body. The constraint preserves the total length of the cable defined as the sum of the Euclidean distance between the attachment points. In addition,

by including the geometry of the fixture in the computation, the constraint can be extended to preserve total torsion between the endpoint. The resulting constraint is relaxed as described in [Lac06] to model the cable elasticity for both overall stretching and torsion. That is, we map the constraint stabilization parameters to physical parameters. The result is two constraint equations generating constraint forces and torques on the set of connected rigid bodies.

The rest of this article is organized as follows. Section 2 provides a brief review of requirements and previous work. Specific contributions of this paper are summarized in section 3. The constraint based elastic cable model is presented in section 4 along with background material on elasticity theory, rigid multibody systems, and integration methods. Validity of the model and associated numerical method is investigated and final results are presented in section 5. Summary and conclusions are found in section 6.

2. Motivation and Background

2.1. Requirements for hoisting cables

The focus of this paper is the real-time numerical integration of mechanical systems involving hoisting cables such as cranes and lifts for instance. An overview on dynamics and control of cranes is found in Ref. [ARNM03]. Characteristically, these systems consist of several movable heavy objects including a load, the crane base, and a movable arm, connected via a light cable with high tension. For most purposes in interactive simulations, the internal dynamics of the cable itself is of less importance compared to the bulk motion of the lifting assembly and load. The most important requirement on the simulated cable is that it shall affect the connected bodies in agreement with the overall elastic behavior described by its length, mass, Young, and torsion modulus. To increase usefulness in interactive simulations, the model should also incorporate the possibility of having the cable sliding over wheels and pulleys, and to let a body slide along the cable to model a ropeway trolley for instance. Finally, as in the case of real hoisting cables, the free length must be allowed to change interactively. This models the effect of a winch. These requirements on the model are important for generating realistic simulations including the many modes of oscillations that hoisting systems may exhibit, and which crane operators and designers must anticipate and control. In addition to the modeling requirements, the dynamics computations should be stable and fast. Interactive applications must drive graphics display at a rate of at least 60 Hz to minimize latencies and this leaves a time budget of less than 16 ms per frame for the entire simulation. On single CPU systems, the numerical integration can only use a small fraction of this, usually of the order of 5 ms.

2.2. Previous work

There are several approaches to cable simulation at interactive rate. We begin by listing different cable models with their advantages and disadvantages.

Lumped Element Models

In these models, the cable is represented by segments, each modeled using either a point particle or a rigid body. Each adjacent pair of bodies is connected with a spring and damper system, a more general force, or with a pairwise constraint. A system of particles with spring-damper forces was applied to surgical thread simulation in [LMGC02] and to virtual prototyping of assembly tasks in [LS01]. A pendulum based on constrained rigid bodies forming a chain is presented in [RGL05]. The lumped element model is intuitively clear and relatively simple and may be realized making use of existing optimized multibody dynamics code, including routines for geometric collision detection. With suitable model for the segment forces the cable will produce accurate dynamics, that may include elastic deformations. A cable made of a simple chain of *particles* with nearest and next-nearest neighbor interactions can however not model twisting resistance as the particles have no orientation, unless complicated forces involving distant neighbors are included. The disadvantage of lumped element based cables is that it is *computationally costly* and *unstable*. When the cable is very stretchy (low spring constant) the computational cost increase linearly with the number of elements as an *explicit* integrator can be used.

However, an explicit integration method quickly becomes inadequate. A short computation for a chain of identical point masses connected with identical springs of stiffness k yields a Young modulus of $k_b = k$ for the cable. Therefore, if we choose n particles per unit length, l_0, the mass of each particle is $m = l_0\rho/n$ and therefore if we keep to Young modulus constant, the natural frequencies increase as $\omega(n) = \sqrt{n}\sqrt{k_b/(l_0\rho)}$, where ρ is the volumetric mass density. Since the time step of an explicit method is usually limited by $\Delta t < \alpha/\omega$, where α is a scalar ($\alpha = 2$ for the Verlet integration scheme), this strategy is limited by both the bulk modulus and the particle density. Hoisting cables are very stiff. For steel cables, for instance, the Young modulus exceeds 200 GPa, the strength is well above 1000 MPa, and the mass density is around 8000 Kg per cubic meter. With these numbers, the spring constant for a typical cable of one square centimeter are is near 20 MN and the mass length density is 0.8 Kg. With 10 particles per meters, say, this leads to oscillations frequencies of approximately 15000 Hz. Using an explicit method such as the Verlet integrator, the time step is then limited to be less than 0.1 ms which means we need at least 10-15 integration steps per frame.

One can use an implicit integration method such as [BW98], or replace the forces by constraints [Bar96] and abandon hope of modeling the stretch dynamics correctly. In

either case, making a time step involves the solving a matrix equation whose size is proportional to the number of segments in the cable. Of course, for cables, these matrices are tightly banded around the main diagonal which speeds things up.

As we explained above, simulating a steel cable supporting only its own weight is typically in itself a stiff problem. But in hoisting systems, the equations are even stiffer since cable segments are typically of much smaller mass than of the load – mass ratios of the order 1/1000 is not uncommon. This increases the oscillation frequencies of the system and as a result, stability becomes difficult to achieve.

Continuum models

Continuum models are based on partial differential equations which are derived from solid mechanics. Stable computational methods for these involve finite elements such as the thin short rods with bending and twisting degrees of freedom of the Cosserat model. This is described described in [Rub00] and applied to surgical simulation by Pai [Pai02]. In Ref. [RNG99], spline objects based on a continuum model are simulated. These models have better theoretical grounding than the lumped element models and there are good numerical methods for them, at least in simple cases of a cable with fixed endpoints as illustrated in [Pai02]. In such cases, the computational cost scales linearly with the cable length and has the benefit of accurately modeling the detailed vibrational, torsional, and bending dynamics. However, cases with contacts, anchor points, and other boundary conditions at locations other than the end point have not been tackled satisfactorily yet. It is expected that these models suffer equally from instability when the mass ratios between the elements and the loads are high.

Constraint based systems

Kinematic constraints express restrictions in the relative motion of physical objects. For instance, a body attached with ball and socket joint at its center of mass can be modeled by the constraint: $x(t) = x(0)$, where $x(t)$ is the Cartesian coordinates of the center of mass.

At first approximation, the net effect on a hoisting wire is to maintain a maximum distance between the the load and the supporting assembly. For the simplest case of a rigid body attached at the center of mass by a cable of fixed length l at a fixed anchor point y, the kinematic constraint is just: $l - \|x - y\| \geq 0$. This is done in [KLM99] for instance where various types of gantry cranes and cables using a Lagrangian formulation which includes pulleys and drivers. Note that the method described in [KLM99] *completely* removes cable stretching, in contrast with the model we propose.

Of course, some internal dynamics can be restored by dividing a cable in segments and connecting these via lumped masses. This is the strategy taken in [KM04] where a single lumped mass other than the load is introduced halfway on the wire. This leads to one extra body and two two body constraints and the added computational cost is small.

When the cable is replaced by a set of distance constraints or with just a few lumped masses, the computational requirement is independent of the cable length and the added cost compared to a system without a cable is just one extra one dimensional two body constraint for each simulated segment. This contrasts with lumped or finite element cable models which may add many 10s of extra degrees of freedom to the system per unit cable length. Provided we have a robust constrained dynamics solver, the bulk effect of the cable can be modeled stably and accurately. Without lumped masses, there is no longer an issue of mass ratio between the load and the cable, but only between the load and the supporting body, i,e., the body the cable constraint is attached to. It is expected however that numerical stability becomes an issue when the lumped masses along the cable are much smaller than the load or the supporting assembly.

The main problem with this approach is the loss of internal dynamics and the ability to model collisions and contacts. Contacts with the cable can be simulated by relocating the lumped masses appropriately at or near the contact points though this was not done in [KM04].

Background summary

From the brief survey presented above, we conclude that there is currently no method for simulating cable for hoisting of heavy objects with satisfactory trade-off between computational speed, stability and accuracy, and modeling flexibility. When full cable dynamics is simulated using lumped or finite element, the computational cost is high and stability under heavy loading is marginal. We note that no one has demonstrated capability of suspending heavy objects with particle or rigid body based cables in real-time. Constraints can do a good job of capturing the essence of cable, i.e., linking heavy objects together and making stable simulation of hoisting systems possible. But the constraint model presented so far are completely rigid and the possibility of extending constrained dynamics to include stiff elastic forces has been overlooked.

3. Contributions of this Paper

The aim here is to construct a method for simulating hoisting cable which is both computationally cheap and capable of modeling the stiff elastic deformations. Because of the small mass ratio between cable and load mass it is reasonable to treat the cables as entirely massless and to replace it with a kinematic constraint. However, the simple two body distance constraint is now replaced with a *multibody* constraint imposing that the *sum* of all length segments between designated body fixed attachment frames add up to the cable length. This departure is significant as one can then measure the pressure exerted by the cable on pulleys which change

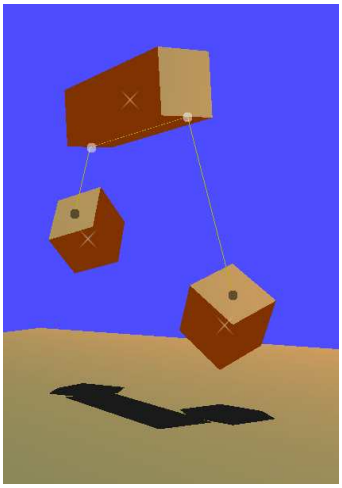

Figure 1: *An illustration of a cable configuration connecting three rigid bodies. The cable has three straight line segments. Dark circles are cable attachment points and the cable is free to slide over the intermediate points marked with bright circles.*

the direction of the cable for instance. This is not possible with models which impose length constraints individually on each segment. The idea is illustrated in Fig. (1) where a single cable connects three bodies. If the attachment points on the rigid bodies also carry an orientation, it becomes also possible to measure the total twist between the end bodies and to compute a restoring torque on these. This is done by imposing a zero net twist between the end points. Bodies are free to slide along the cable as the constraint only imposes conservation of total length.

The second part of the model is the inclusion of cable elasticity by applying a physics based constraint regularization and stabilization scheme. The theory behind constraint regularization is presented in [Lac06]. Using that technique with the right choice of numerical integrator, it is possible to produce fast and robust simulations over a wide range of cable elasticity. It is also possible to include cable velocity constraints to model an engine controlling the rate of change in total cable length and including cable velocity drag. The computational cost of this approach is modest as the complexity is only weakly related to the number of bodies connected to the cable. Indeed, a cable only adds two extra constraints to an existing system including the rest of the crane. Since the bodies connected to the cable are presumed to be already included in the simulation, as opposed to element based methods which add several extra bodies, the only significant computation is the coupling constraint force between the cable and the supporting assembly.

4. Theory

In this section we first describe the theoretical background from elasticity theory and multibody dynamics and then present a constraint based cable that models the interaction of a system of rigid bodies coupled by an elastic massless cable.

4.1. Elasticity theory for cables

Solid mechanics [FT01] provides a theoretical basis for modeling general deformable objects and a specialization to elastic bodies, those which never suffer permanent deformations and the only type we consider here, is covered in [LL86]. Elasticity theory relates geometric deformation–the strain–, with internal force–the stress. Concentrating on ideal, homogeneous and isotropic materials, in the limit of locally small deformation, the stress-strain relation is linear or Hookean, and only depends on two parameters, namely, Young's modulus Y and the Poisson ratio σ. These are easily determined by direct measurements on real materials and can be found listed in many texts on elasticity.

Solid mechanics provides us with dynamical equations that determines the time evolution of a deformable material for given initial conditions, boundary conditions and external forces. Simulations can be built directly from this general theory. Alternatively, one can derive specialized models for elastic solids of specific geometries, such as thin rods. One example of this is Cosserat theory of thin solids [Rub00] with Timoshenko beams as a particular case.

The types of deformation for a thin beam can be grouped into: *stretching*–tangential deformations–, *bending*–curvature deformations–,and *torsion*–twisting deformations. See Fig. (2) for an illustration. A general deformation is a linear combination of these. The internal energies [LL86] associated with these deformations of a cylindrical rod of length L and radius r are

$$U_s = \tfrac{1}{2} c_s \delta x^2 \tag{1}$$

$$U_b = \tfrac{1}{2} c_b \kappa^2 \tag{2}$$

$$U_t = \tfrac{1}{2} c_t \Omega^2 \tag{3}$$

where δx is the elongation, κ is the curvature ($\kappa = R^{-1}$, with radius of curvature R) and twist angle Ω. The constants introduced here are $c_s = AY/L$, $c_b = AYr^2L/4$ and $c_t = AY/4L(1+\sigma)$, where $A = \pi r^2$ is the cross-section area. In the Timoshenko beam theory, valid when the characteristic length scale of deformation–the radius of curvature R–is much larger than the small radius of the beam, the total deformation energy is the sum of these contributions and the force due to a general deformation is the sum of the corresponding three deformation forces.

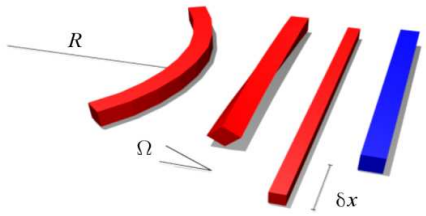

Figure 2: *The three types of deformation for a thin beam: stretching by a length δx, twisting by an angle Ω and bending with a radius of curvature R.*

4.2. The massless cable approximation

A hoisting cable connects a lifting device, such as a crane, with a load mass M which is typically much larger than the cable mass m. Mass ratios $m/M \approx 1/1000$ are not uncommon for steel wires. The massless cable approximation that we suggest consists of discarding cable mass and internal dynamics but incorporating the effect of coupling an arbitrary number of rigid bodies together. This preserves the net effect of cable tension accurately models elasticity as well. See Fig. (1) for an example of a cable and rigid body system. The cable is modeled with a constraint and the elasticity properties are simulated using properties is modeled using constraints and elasticity is modeled using constraint regularization and mapping the parameters to the cable internal energies of Timoshenko beams. This is further developed in the sections below. Bending deformations can be neglected in hoisting cables as the corresponding forces are small in comparison to the cable tension. In addition, for hoisting cable supporting large masses, bending deformations are localized to a small region along the cable. Therefore this type of deformation is part of the cable internal dynamics and cannot be treated by this cable model that carries no local information.

Some dynamics is lost in making the massless cable approximation. *i)* The cable inertia is neglected. The effect on the motion of the load and crane is minute. The contribution of the cable mass to the time period of a swinging load is of the order $\sqrt{m/M}$ and can be compensated for by increasing the load mass. *ii)* The cable's internal dynamics is lost. Although the light cable has vibrational modes, the frequencies of these are factor $\sqrt{M/m}$ higher than that of the crane-load system. This discrepancy in time scale results in that the cable internal dynamics is only weakly coupled to the motion of the crane and load. The gain of this approximation, on the other hand, is a computationally efficient method that well describes dynamics of the load and crane.

4.3. Multibody dynamics

Here we summarize the main results of multibody dynamics that are needed for us. We make extensive use of dense matrix formulation. We refer to Baraff [Bar96] and Erleben [ESHD05] for further reading on multibody dynamics for visual interactive simulations.

We use the following notation. The state vector of the multibody system of N rigid bodies is $(q^T, v^T)^T$ with respect to the global inertial frame. $q = (q^{T(1)}, q^{T(2)}, \ldots, q^{T(N)})^T$ contains the generalized coordinate vectors $q^{(i)} = (\mathbf{x}^{T(i)}, e^{T(i)})^T$, where $\mathbf{x}^{(i)}$ is the center of mass position vector of body (i) and $e^{(i)}$ is a unit quaternion defining the orientation of the body. The velocities are represented by $v = (v^{T(1)}, v^{T(2)}, \ldots, v^{T(N)})^T$, where $v^{(i)} = (\dot{\mathbf{x}}^{T(i)}, \omega^{T(i)})^T$ for body (i) and with the angular velocity vector denoted by $\omega^{(i)}$. With these representations we have the relation $\dot{q}^{(i)} = T(q^{(i)})v^{(i)}$, where $T(q^{(i)}) = \mathrm{diag}(I, \tilde{T}(e^{(i)}))$, I is the 3×3 identity matrix and

$$\tilde{T}(e) = \frac{1}{2}\begin{pmatrix} -e_1 & -e_2 & -e_3 \\ e_0 & e_3 & -e_2 \\ -e_3 & e_0 & e_1 \\ e_2 & -e_1 & e_0 \end{pmatrix} \tag{4}$$

The body mass $m^{(i)}$ and body inertia tensor $\mathcal{I}^{(i)}$ in global frame are collected into the mass matrix $M^{(i)} = \mathrm{diag}(m^{(i)}I, \mathcal{I}^{(i)})$ and we form the system mass matrix as $M = (M^{(1)}, M^{(2)}, ..., M^{(N)})$. In terms of the body frame inertia tensor $\mathcal{I}_0^{(i)}$, the inertia tensor with respect to the global inertial frame is $\mathcal{I}^{(i)} = R^{(i)}\mathcal{I}_0^{(i)}R^{T(i)}$, where $R^{(i)} = R^{(i)}(e^{(i)})$ is the rotation matrix of body (i).

Non-dissipative forces can be introduced by assigning potential energy to the system, $U(q,t)$. The corresponding force is $F = -T^T \partial U/\partial q^T$. The equations of motion for the multibody system are the Newton-Euler equation of motion

$$M\dot{v} = F_M + F \tag{5}$$

where we have introduced notation for the gyroscopic force $F_M = -\dot{M}v$. For each rigid body (i) we can read off the equation $M^{(i)}\dot{v}^{(i)} = F_{M^{(i)}} + F^{(i)}$, where $F_{M^{(i)}} = -\dot{M}^{(i)}v^{(i)}$ and $F^{(i)} = -T^{T(i)}\partial U/\partial q^{T(i)}$.

4.3.1. Constrained dynamics

The constraints represent the net effect of the dynamics on short time and length scales that is intractable to simulate directly. For reading on constrained multibody dynamics, see Refs [Bar96] and [WGW90].

We begin by considering kinematic constraints, i.e., constraints for the generalized coordinates q. We also restrict ourselves to holonomic constraints, i.e., constraints that can

be expressed as $\phi(q,t) = 0$, but we allow them to be explicitly time-dependent (rheonomic constraints). Given these restrictions we have excluded velocity constraints, like linear and angular drivers, and contact constraints. In Section 4.3.3 we extend to include also velocity constraints.

A constraint $\phi(q,t) = 0$ specifies a surface in the general coordinate space. The system coordinates q are thus restricted to always belong to this, possibly time-dependent, surface. The constraint force, acting to keep q on the surface $\phi(q,t) = 0$, is $F_c = G^T\lambda$, where $G = (\partial\phi/\partial q^T)T(q)$ is the constraint Jacobian and λ is the Lagrange multiplier. The constraint force is directed orthogonal to the constraint surface and the magnitude depends on the shape of the constraint surface at the present position, the velocity of the bodies and the other forces acting on the system. The equations of motion are appended with the equation $\phi(q,t) = 0$. With the inclusion of constraints the system is no longer an ordinary differential equations (ODE), but instead, a differential algebraic equation (DAE). DAEs are more difficult to integrate numerically – one common difficulty is to prevent numerical drift of ϕ away from 0 and simultaneously preserving the systems total energy.

By differentiating the constraint $\phi(q,t) = 0$ with respect to time, we note that $0 = \dot{\phi} = Gv + \partial\phi/\partial t$. The work done by the constraint force on the system is the integral of: $F_c^T v = \lambda^T Gv = -\lambda^T \partial_t \phi$. When the constraint has no explicit time-dependence the system is closed and the work exerted by the constraint force is zero. In general, time-dependent constraints result in non-zero work on the system by the constraint force, indicating that the system is non-closed – external interactions are present. In our case, this could be a cable where the total length is varied, e.g., by running a winch.

In a system with N_c constraints we use the representation $\phi = (\phi^{T[i]}, \phi^{T[2]}, \ldots, \phi^{T[N_c]})^T$, where $\phi^{[i]}$ is the i:th constraint, that may be of dimension $d^{[i]} = 1, 2, \ldots, 6$ and involve any number of bodies. The dimension of ϕ is thus $\dim(\phi) = \sum_i d^{[i]} \equiv d_c$. The dimension of the system Jacobian is then $\dim(G) = d_c \times 6N$ and the dimension of the Lagrange multiplier is $\dim(\lambda) = d_c$.

4.3.2. Constraints and strong potentials

Here we describe the relation between constraints and potentials. This is useful in designing a real-time model for cables, where the cable elasticity can range from very stiff to highly elastic and with stable integration of the motion. The transition from constraints to strong potentials is referred to as *constraint regularization* [Lac06].

Say that the system potential can be represented as

$$U(q) = \tfrac{1}{2}\phi^T(q)\varepsilon^{-1}\phi(q)$$

for some d_c-dimensional vector function $\phi(q)$ and real positive diagonal matrix ε of dimension $d_c \times d_c$. Note that the cable energies in Eqs. (1)-(3) are of this form. The contribution to the generalized force of this potential takes the form

$$F_\phi = -G^T\varepsilon^{-1}\phi$$

If $\phi(q) = 0$ at $t = 0$, the solution converges uniformly, as the diagonal terms $\varepsilon_{ii} \to 0$, towards the exactly constrained solution where $\phi(q) = 0$ for $t > 0$. Note that when the artificial variable $\lambda = -\varepsilon^{-1}\phi$ is introduced the generalized force can be written $F_\phi = G^T\lambda$ and the equations of motion are modified to

$$\dot{q} = T(q)v \tag{6}$$

$$M\dot{v} - G^T\lambda = F_M + F \tag{7}$$

$$\varepsilon\lambda(q,t) = -\phi(q,t) \tag{8}$$

This particular form of the equations is useful when it comes to discretizing the system and finding a stable integrator. Observe that if the constraint is formulated on the potential form with a physically based potential energy, constraint regularization automatically results in a physical forces and the stiffness of the force may be varied from highly soft (large ε) to very stiff (small ε).

4.3.3. Velocity constraints

It is useful to also include velocity constraints. These can be used for modeling drivers. In our case a driver could be an engine controlling the rate of change of cable length in the system. The time derivative of a kinematic constraint implies

$$0 = \Gamma(q,v,t) \equiv Jv - w(t) \tag{9}$$

where we denote $w(t) \equiv -\partial\phi/\partial t$. We take this as our velocity constraint. The velocity constraint introduces a second Lagrange multiplier ρ and constraint force $F_\Gamma = J^T\rho$. Velocity constraints can be regularized by introducing a Rayleigh's dissipation function $\mathcal{R} = \frac{1}{2}\Gamma^T\xi^{-1}\Gamma$, where ξ is a real positive diagonal matrix, such that $F_\Gamma = -\partial\mathcal{R}/\partial v^T = -J^T\xi^{-1}\Gamma$. Note that ξ cannot be deduced from cable material parameters alone. It is a parameter that models the design of the driving engine and the friction in the system – parameterizing slipping of the cable that is connected to the driver. The equations of motion (6)-(8) are thus modified by the contribution of $J^T\rho$ to the generalized force and the algebraic equation for the new variable ρ

$$\xi\rho = -\Gamma(q,v,t) \tag{10}$$

4.3.4. Numerical integration

When it comes to time stepping of the system, stability and speed of computation are more important than high accuracy. This leaves essentially three usable choices: fully explicit using the Verlet Leapfrog method, fully implicit using (linearized) backward Euler or the midpoint scheme, or semi-implicit time integration. Fully explicit Verlet time

stepping combined with moderate spring forces is the cheapest choice. This technique has been popular for ropes and cloth. But for any mass-spring systems, there is an *upper limit for the spring stiffness* for each size of time step, as explained in section 2.2. Above this limit the simulation becomes unstable. Linearly implicit integration allows larger stiffness and larger time steps. This involves solving a linear system of equations at each time step and depending on the configuration of the system, this can be a reasonable cost, especially if iterative methods are used as in [BW98]. But linearly implicit integration also introduces artificial damping that drains the energy from the system even to the extent that the force is significantly inaccurate both in size and direction. For instance, a 2D pendulum with a stiff spring integrated with linear implicit Euler do not swing at the correct rate under gravity because of this artificial damping, see Ref. [Lac06]. The error, may be very large and depends on time step and stiffness. Stability may instead be achieved by replacing the stiff forces by constraints in combination with explicit or semi-implicit integration. We follow this route. Employing a Verlet-Leapfrog discretization of Eqs. (6)-(8) with the velocity constraint (10) included, and the Taylor expansion $\phi(x_{n+1}) = \phi(x_n) + \frac{\partial\phi(x_n)}{\partial x_n}(x_{n+1} - x_n) + ... \approx \phi_n + \Delta t G_n v_{n+1}$ gives after rearranging some Δt factors

$$q_{n+1} = q_n + \Delta t T(q_n) v_{n+1} \tag{11}$$

$$\mathbb{A}_n u_{n+1} = b_n \tag{12}$$

with

$$\mathbb{A}_n = \begin{pmatrix} M & -\tilde{G}_n^T \\ \tilde{G}_n & \Delta t^{-2}\tilde{\varepsilon} \end{pmatrix} \tag{13}$$

and $\tilde{G} = (G^T, J^T)^T$, $\tilde{\varepsilon} = \mathrm{diag}(\varepsilon, \xi)$, $u_{n+1} = \Delta t(v_{n+1}^T, \lambda_{n+1}^T, \rho_{n+1}^T)^T$ and $b_n = (Mv_n^T + \Delta t(F_n^T + F_{Mn}^T), -\Delta t^{-1}\phi_n^T, -\Delta t^{-1}\Gamma_n^T)^T$. Note that in this system, the discrete value of λ_n, ρ_n are actually *average* values over the time step, as is needed to avoid non-convergent high frequencies in the limit of $\varepsilon \to 0$. We solve this linear system by first building the Schur complement, $\tilde{G}M^{-1}\tilde{G}^T + \Delta t^{-2}\tilde{\varepsilon}$, and solve for the Lagrange multiplier and then compute the velocity and finally update the positions. Observe that there is no singularity for $\tilde{\varepsilon} = 0$ – it can be taken arbitrarily small. The velocity constraint (or the length and twist constraint) can be left out by simply discarding the variable ρ (or λ) and setting $\tilde{G} = G$ and $\tilde{\varepsilon} = \varepsilon$ (or $\tilde{G} = J$ and $\tilde{\varepsilon} = \xi$).

4.4. Cable constraint

We introduce massless cables in the model as a kinematic constraint. The constraints are then relaxed and made elastic. The number of bodies connected by the constraint may be arbitrary, but larger or equal to two. Say the cable is divided into J segments of straight lines, each of length $l_1, l_2, \ldots, l_J$. See Fig. (3) for an illustration. The lines connect the cable nodes $j = 1, 2, \ldots, J+1$. The positions of the nodes in world frame are denoted $\mathbf{p}_1, \mathbf{p}_2, \ldots, \mathbf{p}_{J+1}$. A node j is an attachment point on a body indexed by (i), such that $\mathbf{p}_j = \mathbf{x}^{(i)} + \mathbf{d}_j$, where $\mathbf{d}_j$ is a body fix vector giving the node position relative to the center of mass of body (i). At the first and last node the cable is held fixed relative to the body (or to the world frame). The cable is free to slide and rotate over the intermediate nodes. As a result, the individual segment lengths l_j may vary. We define the cable twist angle by $\Omega \equiv \Omega^{(a)}_{\mathbf{d}_1} + \Omega^{(b)}_{\mathbf{d}_{J+1}}$, where (a) and (b) are the body indexes of the cable's first and last attachment points and $\Omega^{(i)}_{\mathbf{d}_j}$ is the angle of rotation of body (i) about the body fix vector $\mathbf{d}_j$, see Fig. (3). As pointed out before, we discard from bending resistance as this is not applicable to hoisting systems. For an *ideally stiff* cable, the constraint enforced by the cable on the bodies is that *the sum of segment lengths should equal the total cable length* $L(t)$ and that *the cable should not be twisted*. In mathematical terms the cable constraint is $0 = \phi = (\phi_s^T, \phi_t^T)^T$, with

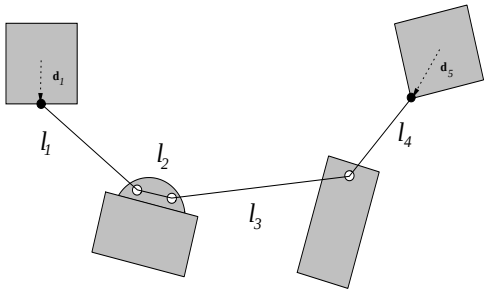

Figure 3: *A figure illustrating a massless cable connecting four rigid bodies. The cable has four straight line segments. Colored circles mark the cable attachment points. The cable is free to slide over the intermediate points marked with open circles as long as the total length is maintained. The twist angle is defined through the orientation of the bodies at the start and end point of the cable about the body fix vectors* $\mathbf{d}_1$ *and* $\mathbf{d}_5$.

$$\phi_s \equiv \sum_{j=1}^{J} l_j - L(t) \tag{14}$$

$$\phi_t \equiv \Omega \tag{15}$$

Observe that ϕ_s and ϕ_t coincides with δx and Ω in the expressions for the cable internal energies in Eqs. (1) and (3). The stretch constraint in Eqn. (14) restricts the motion of the bodies to preserve the total length of the cable, $L(t)$. This length may be interactively altered – corresponding to releasing more cable, say from a winch. The no-twist constraint, Eqn. (15), affects only the bodies connected to the cable endpoints – if body (a) is rotated an angle $\Omega^{(a)}_{\mathbf{d}_1}$ about $\mathbf{d}_1$ body (b) must be rotated the opposite amount, $\Omega^{(b)}_{\mathbf{d}_{J+1}} = -\Omega^{(a)}_{\mathbf{d}_1}$ about $\mathbf{d}_{J+1}$.

4.4.1. Jacobian

The cable constraint $0 = \phi = (\phi_s^T, \phi_t^T)^T$ has dimension 2. The Jacobian is $G = (G_s^T, G_t^T)^T = (\partial\phi/\partial q^T)T^T$ and has dimension $2 \times 6N$. We begin with deriving the Jacobian for the stretch constraint. The time derivative takes the form $0 = \dot{\phi}_s = G_s v - \dot{L}$. We identify the explicit form of the Jacobian by computing the time derivative of the constraint. Note first that any segment j has length $l_j = \|\mathbf{p}_j - \mathbf{p}_{j+1}\|$, with $\mathbf{p}_j = \mathbf{x}^{(a)} + \mathbf{d}_j$ and $\mathbf{p}_{j+1} = \mathbf{x}^{(b)} + \mathbf{d}_{j+1}$ for bodies (a) and (b) connected by the segment. The time derivative of l_j is

$$\dot{l}_j = \mathbf{k}_j \cdot (\mathbf{v}^{(a)} - \mathbf{v}^{(b)}) - (\mathbf{k}_j \times \mathbf{d}_j) \cdot \omega^{(a)} + (\mathbf{k}_j \times \mathbf{d}_{j+1}) \cdot \omega^{(b)}$$

where $\mathbf{k}_j = (\mathbf{p}_j - \mathbf{p}_{j+1})/\|\mathbf{p}_j - \mathbf{p}_{j+1}\|$. The time derivative of ϕ equals the sum of the segments length, $\dot{l}_j$, minus $\dot{L}$. We identify the Jacobian

$$G_s = \sum_{j=1}^{J} \left(\ldots, \mathbf{k}_j^T, -(\mathbf{k}_j \times \mathbf{d}_j)^T, \ldots, -\mathbf{k}_j^T, (\mathbf{k}_j \times \mathbf{d}_{j+1})^T, \ldots \right) \tag{16}$$

where the positions in the Jacobian are those of $v^{(a)} = (\mathbf{v}^{T(a)}, \omega^{T(a)})^T$ and $q^{(b)} = (\mathbf{v}^{T(b)}, \omega^{T(b)})^T$ in v.

Next we derive the Jacobian for the twist constraint, Eqn. (15). We identify the Jacobian from the time derivative of the twist constraint, $0 = \dot{\phi}_t = G_t v$. To determine the angle of rotation about the body fixed vector $\mathbf{d}$, we convert from quaternion to Euler angles. For the Euler angles Roll (Φ), Pitch (Θ) and Yaw (Ψ) we use the XYZ-convention such that the rotation matrix reads $R(\Phi, \Theta, \Psi) = R_z(\Phi)R_y(\Theta)R_x(\Psi)$. If we let the local body frame be defined such that $\mathbf{d}$ is aligned to the x-axis, the rotation angle about $\mathbf{d}$ is given by the Yaw angle Ψ. The twist angle should be allowed to exceed one evolution. Thus we must also keep track of the winding number η. We then have the following expression for the twist angle

$$\Omega = \Omega_{\mathbf{d}_1}^{(a)} + \Omega_{\mathbf{d}_{J+1}}^{(b)} = \Psi^{(a)} + \Psi^{(b)} + \eta 2\pi \tag{17}$$

where $\Psi^{(i)} = \arctan(f^{(i)})$ and $f \equiv R_{32}(e)/R_{33}(e) \equiv 2(e_0 e_1 + e_2 e_3)/[1 - 2(e_1^2 + e_2^2)]$. By the chain rule it follows that

$$\dot{\Psi}^{(i)} = \mathcal{A}^{T(i)} \omega^{(i)} \tag{18}$$

where (omitting the body index (i) temporarily)

$$\mathcal{A} \equiv \frac{R_{33}^{-1}}{1 + f^2} \left[\frac{\partial R_{32}}{\partial e^T} \tilde{T} - f \frac{\partial R_{33}}{\partial e^T} \tilde{T} \right] \tag{19}$$

We identify the twist Jacobian as

$$G_t = \left(\ldots., 0^T, \mathcal{A}^{T(a)}, \ldots., 0^T, \mathcal{A}^{T(b)}, \ldots. \right) \tag{20}$$

with again the positions in the Jacobian being those of $v^{(a)}$ and $v^{(b)}$ in v.

It should be noted that the twist measure is not entirely free from singularities. Care should be taken when $R_{33} \to 0$, while it should be pointed out that G_t remains finite although f diverges. The only severe singularity occurs when $\mathbf{d}$ becomes co-aligned with cable, i.e., when the body center point lies on the connecting cable segment–a case that seldom occurs for hoisting systems, and does not occur at all when cable-body collision is taken into consideration.

4.4.2. Modeling elasticity with regularized constraints

We introduce elasticity in the system through constraint regularization

$$\phi \to U = \frac{1}{2} \phi^T(q) \varepsilon^{-1} \phi(q) \tag{21}$$

with $\text{diag}(\varepsilon) = (c_s^{-1}, c_t^{-1})$. With the constraint defined as in Eqs. (14) and (15) this reproduces the cable internal energies in Eqs. (1) and (3). For appropriate values of the material parameters and geometrical dimensions this accurately models the stretching and torsional resistance of the cable. The material parameters for a steel cable, for instance, are roughly $Y = 200 \cdot 10^9 Pa$ and $\sigma = 0.3$. For a circular steel cable of diameter 10 *mm* end length 4 *m*, the regularization parameters are $c_s \approx 7.8 \cdot 10^6\ N/m$ and $c_t \approx 19\ Nm/rad^2$.

5. Results

We propose and investigate massless cable as an alternative to dynamically modeled cable. The main results of this paper are, besides the theoretical framework presented above, validation tests and the computational efficiency and stability of the method. We also demonstrate the method for a more complex system and the feature of velocity driver.

5.1. Model validation

The physical model is the elastic deformation energies for Timoshenko beams in Eqs. (1) and (3). To validate the model we first consider a simple setup with two boxes and one cable, as demonstrated in Fig. (4). In the validation tests the boxes are given an initial linear or angular velocity. In all of the tests the boxes have the mass 1000 Kg, side length 2 *m*, the cable length is 4 *m* and the time step used is $\Delta t = 0.01$ *s*. Gravity is set to zero in the validation tests. Results of the stretch tests, initialized with a linear velocity, are presented in Fig. (5) for three different values of c_s: 10, 10^3 and $10^6 N/m$. The twist tests, initialized with a angular velocity, are presented in Fig. (7) for three different values of c_t: 10, 10^3 and $10^6 Nm/rad^2$. Observe that the twist angle may exceed one evolution. The values of ϕ_s (and ϕ_t) are plotted as functions of time together with the elastic force $f_{\phi_s} = G_s^T \lambda_s$ normalized by c_s (and torque $f_{\phi_t} = G_t^T \lambda_t$ normalized by c_t) that is associated with the assigned energies. These coincides very well, confirming that the internal deformation energies we have assumed for the system produces the elastic forces. The oscillation time periods match the theoretically expected values: 44 *s*, 4.4 *s* and 0.14 *s* (stretch tests) and 36 *s*, 3.6 *s*

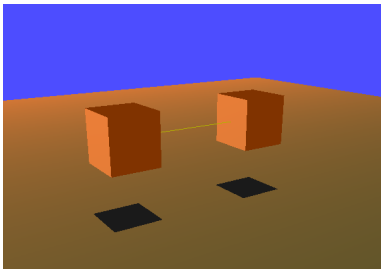

Figure 4: *The validation system. We consider two rigid bodies connected by a cable. The system is initialized with linear and angular velocities to validate the cable stretch and twist elasticity.*

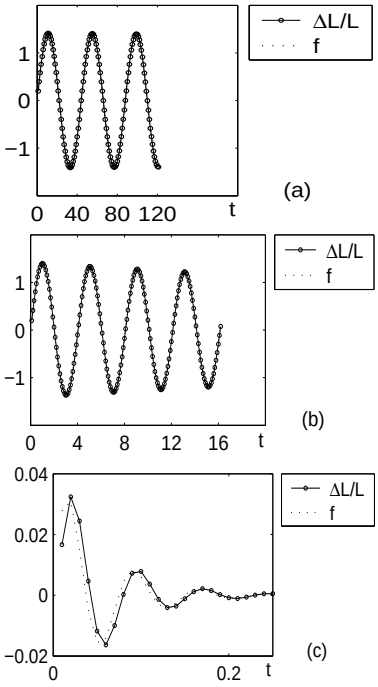

Figure 5: *Stretch validation tests displaying the variation in cable length, $\Delta L/L$, and stretch force normalized by c_s as a function of time and for different stretch resistance: c_s: 10 (a), 10^3 (b) and 10^6 (c).*

and 0.11 *s* (twist tests) except for very large constants, e.g., $c_t = 10^6$, where the motion is strongly damped. The damping is clearly seen in the energy plots in Fig. (6) and Fig. (8). This is due to the numerical integration scheme we have chosen. It should however be emphasized that the dissipation here affects only the *vibrational motion*, as opposed to using linearized implicit Euler integration of the dynamical equations with the elastic forces included directly, which is the more conventional approach and may damp *all motion*. It is from these results clear that elastic forces in the cable follows the physical laws that we have imposed, apart from numerical damping and thereby slight shift in oscillation frequency for very stiff materials. The time stepping is clearly stable for these test setups.

5.2. Computational efficiency

What is the computational cost for massless cables and how does this scale with the number of bodies? In each time step the constraint force is computed by first solving a linear system involving the Schur complement of $\mathbb{A}$ in Eqn. (13). For simplicity we exclude the cable velocity constraint, here. For a system involving no other constraints but a single massless cable the Schur complement, $GM^{-1}G^T + \Delta t^{-2}\varepsilon$, has dimension 2×2 and is inverted at virtually no cost. Observe that this holds *irrespectively of the number of bodies connected to the cable*. For any reasonable system, massless cables will not be a computational bottle neck and we therefore do not present any timing results. Massless cable should be compared to the alternative – rigid body (or particle) based cables, where N_s bodies, pairwise connected with in total $N_s - 1$ constraints each of dimension between 3 to 6, make up the cable. To this number we should also add n constraints connecting the cable with the other bodies in the system resulting in $d_{cable} = 3(N_s - 1 + n)$. The resulting size of the Schur complement for rigid body based cable is $d_{cable} \times d_{cable}$. Contrary to massless cable. this has potential of being the most computationally costly part of the simulation, especially since the integration is complicated by stability issues due to the small cable-load mass ratio.

The result is similar when it comes to adding a cable to an already constrained system, e.g., a crane construction. Say that the system not including the cable has constraints of total dimension summing to d_c, e.g., ball constraints, hinges etc. Computing the constraint forces involves solving a matrix equation involving the Schur complement matrix of dimension $d_c \times d_c$. Adding a *massless cable* to this system increases the matrix size to $(d_c+2) \times (d_c+2)$ whereas adding a *rigid body based cable* increases the matrix size to $(d_c + d_{cable}) \times (d_c + d_{cable})$. The computational cost for solving the matrix equation scales as between $O((d_c + d_{cable})^1)$ to $O((d_c + d_{cable})^3)$ depending on the sparsity pattern of the Schur complement and solver strategy. Typically $d_{cable} \gg 2$ and it is not unreasonable to expect $d_{cable} \gg d_c$.

5.3. Demonstration

We also consider a more complex system to demonstrate how the massless cable constraint can be utilized, see Fig. (9). This example consists of four cables and six rigid bodies with masses ranging between $1 - 100$ Kg, gravity $g = 10\ m/s^2$, cable elasticity c_s between $10^3 - 10^7$ and with cable lengths between 1-30 m. The two smaller boxes are connected by a single cable that slides freely over two attachment points on the larger box above, like a pulley. The ca-

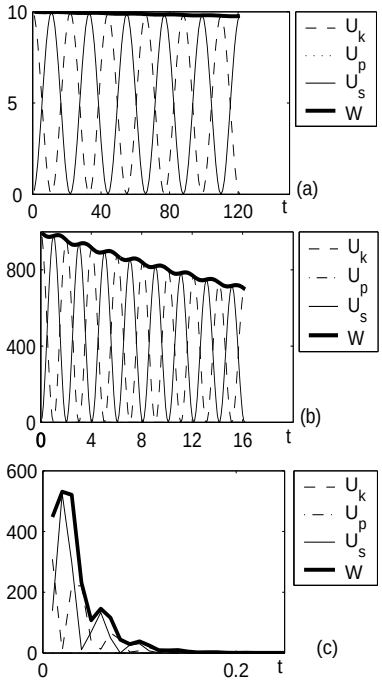

Figure 6: *Energy variation in the stretch validation tests as a function of time and for different stretch resistance: c_s: 10 (a), 10^3 (b) and 10^6 (C). W is the total energy, i.e., the sum of kinetic energy U_k, potential energy U_p (e.g., due to gravity) and constraint energy U_s.*

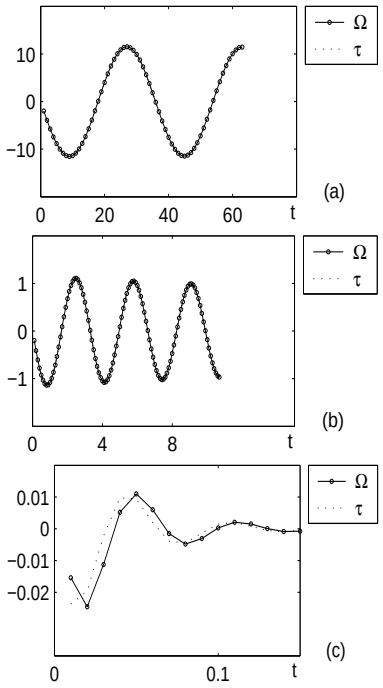

Figure 7: *Twist validation tests displaying the twist angle, Ω, and cable torque normalized by c_t as a function of time and for different twist resistance: c_t: 10 (a), 10^3 (b) and 10^6 (c). Observe that the twist may exceed one revolution, see figure (a).*

ble twist resistance couples the orientation of the two small boxes and forces them to rotate in opposite directions, but with some elasticity. The torsional elasticity c_t is here set to 10. The wider body on top slides freely along the two horizontal cables. Two static boxes are connected to the world by a lock constraint. The system is integrated with time step $\Delta t = 0.05$ *s* and shows stable behavior with slight energy dissipation in the cable oscillations. This system would have been difficult to simulate in real-time using any lumped element model for the cable as. Such a simulation would require considerably more than the six elements already included and, besides performance the issue, there would have been difficulties with smooth cable sliding and problems with obtaining stability despite large mass ratios in the system.

The velocity constraint is demonstrated by Fig. (10) from a simulation where a box of mass 1 Kg and initially is tossed away from a rod of mass 0.02 Kg with one point nailed at height 12 *m* by a spherical constraint. By setting a driving velocity on the cable connecting the objects the box is then re-winded. The friction and driving cable velocity has three different values during the simulation: $\xi = 10$ and $w = 0$ during the toss, $\xi = 0.1$ and $w = -0.2$ during the rewinding and larger friction and driving velocity $\xi = 0.05$ and $w = -0.5$ during the lifting of the box to overcome the cable slipping. In this simulation the length velocity constraint is the only cable constraint that is included.

6. Summary and Conclusions

We have presented a technique for efficient and stable simulation of hoisting cable. The idea is to use, instead of costly dynamically simulated cable, a cable model free of internal dynamics but capable of connecting several bodies under stiff elastic length and twist forces.

In Eq. (14) and (15) we present a constraint representing a *single* massless cable that connects an *arbitrary number of bodies*. The cable constraint preserves the total length of the cable, that may be interactively varied, and the cable twist angle. The resulting constraint Jacobian is given in Eq. (16) and (20). By constraint regularization based on the internal energies of an elastic cable it is possible to make stable real-time simulation of complex hoisting systems with cable elasticity ranging from highly elastic to very stiff and with large load masses.

The computational cost is negligible for any reasonable system, and is in particular much cheaper than dynamically

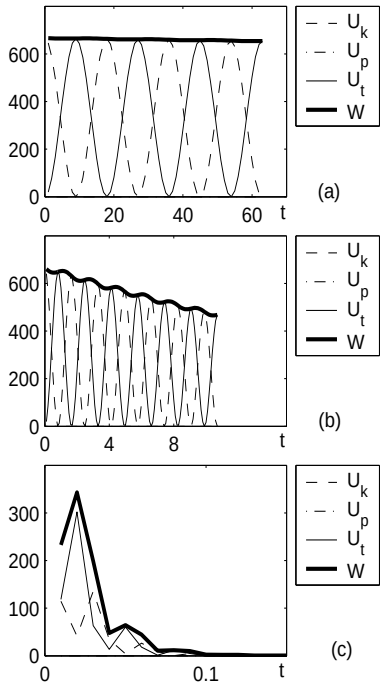

Figure 8: *Energy variation in the twist validation tests as a function of time and for different twist resistance: c_s:* 10 *(a),* 10^3 *(b) and* 10^6 *(c). W is the total energy, i.e., the sum of kinetic energy U_k, potential energy U_p (e.g., due to gravity) and constraint energy U_t.*

simulated cables, see Sec. 5.2. The presented model is also attractive from the design point of view – the cable is defined by its start and end points plus intermediate sliding points, representing pulleys and wheels, and the elasticity parameters are directly related to well-known material parameters, such as the Young's modulus. For most hoisting systems it is not reasonable to simulate all cables dynamically, because of the high computational cost and poor stability properties. Massless cable is then an alternative that produces stable simulations at low computational cost but still models elastic stretching and twisting.

The presented method requires some extensions to be fully useful in applications. When the load is resting, e.g., on the ground and the tension in the cable drops, the cable should allow to slack, .i.e., bend under its own weight due to gravity. This can be achieved by switching between the massless cable model and a dynamic cable model, based on light particle or rigid body segments – in the slacking mode these can be integrated with large time steps and with computationally cheap methods. Furthermore, collision between cables and rigid bodies and cables with cables should also be included. The massless cable model can be extended to include this. When collision is detected, extra cable nodes can

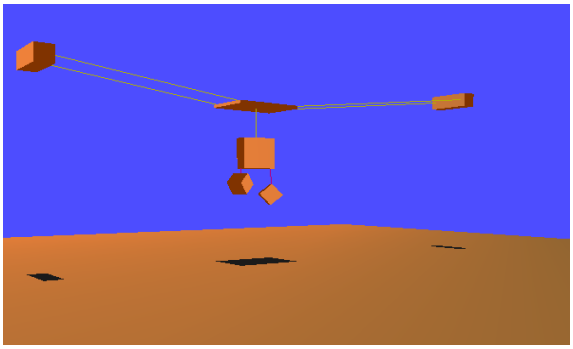

Figure 9: *Snapshot from a simulation of a more complex system involving four cables. The two smaller boxes are connected by a single cable running through the box above them, like a pulley. The twist resistance enforces the two smaller boxes to rotate in opposite directions. The larger body on top slides freely along the two horizontal cables.*

be inserted at the collision point. These cable nodes should not be fixed to the body but move along the surface of the body, always taking the position that minimizes the cable length.

7. Acknowledgments

The research was supported in part by ProcessIT Innovations, "Objective 1 Norra Norrlands" EU grant awarded to HPC2N/VRlab at Umeå University and by the Swedish Foundation for Strategic Research (SSF-A3 02:128).

References

[ARNM03] ABDEL-RAHMAN E. M., NAYFEH A. H., MASOUD Z. N.: Dynamics and control of cranes: A review. *Journal of Vibration and Control 9*, 7 (2003), 863–908.

[Bar96] BARAFF D.: Linear-time dynamics using lagrange multipliers. In *SIGGRAPH '96: Proceedings of the 23rd annual conference on Computer graphics and interactive techniques* (New York, NY, USA, 1996), ACM Press, pp. 137–146.

[BW98] BARAFF D., WITKIN A.: Large steps in cloth simulation. In *SIGGRAPH '98: Proceedings of the 25th annual conference on Computer graphics and interactive techniques* (New York, NY, USA, 1998), ACM Press, pp. 43–54.

[ESHD05] ERLEBEN K., SPORRING J., HENRIKSEN K., DOHLMANN H.: *Physics-based Animation*. Charles River Media, Aug. 2005.

[FT01] FUNG Y. C., TONG P.: *Classical and Computational Solid Mechanics*. World Scientific, Singapore, 2001.

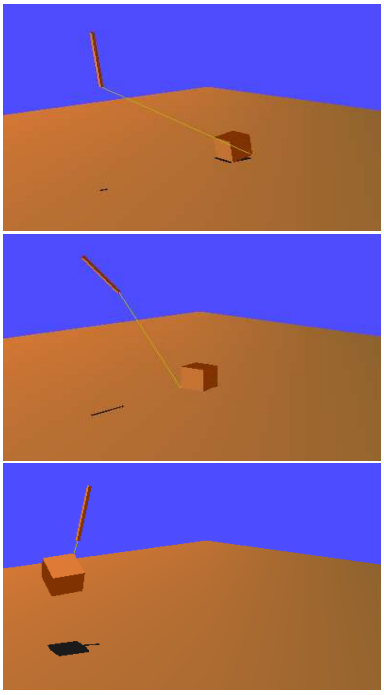

Figure 10: *Snapshots from a simulation of a system similar to a fishing rod, illustrating the use of the cable velocity constraint. The box is initially tossed away (top figure), then re-winded (middle figure) and finally lifted (bottom figure) by setting a driving velocity on the cable. In the lifting stage the friction in the driver is increased to overcome the cable slipping.*

[KLM99] KISS B., LÉVINE J., MÜLLHAUPT P.: Modelling, flatness and simulation of a class of cranes. *Periodica Polytechnica Electrical Engineering, 43*, 03 (1999), 215–225.

[KM04] KANG S.-C., MIRANDA E.: Physics based model for simulating the dynamics of tower cranes. *International Conference on Computing in Civil and Building Engineering, ICCCBE, Weimar, Bauhaus-Universität, Germany 10* (2004), 248–253.

[Lac06] LACOURISÈRE C.: A regularized time stepper for multibody simulations. *Internal report, UMINF-106.04, issn 0348-0542, URL: www.cs.umu.se/research/reports* (2006).

[LL86] LANDAU L., LIFSCHITZ E.: *Theory of Elasticity*. Pergamon Press, Oxford, 3rd ed, 1986.

[LMGC02] LENOIR J., MESEURE P., GRISONI L., CHAILLOU C.: Surgical thread simulation. *Modelling and Simulation for Computer-aided Medecine and Surgery (MS4CMS), EDP Sciences. 12* (2002), 102–107.

[LS01] LOOCK A., SCHÖMER E.: A virtual environment for interactive assembly simulation: From rigid bodies to deformable cables. In *5th World Multiconference on Systemics, Cybernetics and Informatics (SCI'01), Vol. 3 (Virtual Engineering and Emergent Computing)* (2001), pp. 325–332.

[Pai02] PAI K.: Strands: Interactive simulation of thin solids using cosserat models. *Computer Graphics Forum 21*, 3 (2002), 347–352.

[RGL05] REDON S., GALOPPO N., LIN M. C.: Adaptive dynamics of articulated bodies. *ACM Trans. Graph. 24*, 3 (2005), 936–945.

[RNG99] RE'MION Y., NOURRIT J.-M., GILLARD D.: Dynamic animation of spline like objects. In *WSCG'99 Conference Proceedings* (1999), Skala V., (Ed.), pp. 426–432.

[Rub00] RUBIN M. B.: *Cosserat Theories: Shells, Rods and Points*. Kluwer Academic Publ., Dordrecht, 2000.

[WGW90] WITKIN A., GLEICHER M., WELCH W.: Interactive dynamics. *Computer Graphics 24*, 2 (1990), 11–21.